Environmental Science

AIMS Environmental Science, 11(3): 381–400.
DOI: 10.3934/environsci.2024019
Received: 22 March 2024
Revised: 22 May 2024
Accepted: 24 May 2024
Published: 31 May 2024

http://www.aimspress.com/journal/environmental

Research article

Exploration of bacterial strains with bioremediation potential for mercury and cyanide from mine tailings in "San Carlos de las Minas, Ecuador"

Cristina Calderón-Tapia[1,*], Edinson Medina-Barrera[2], Nelson Chuquin-Vasco[3], Jorge Vasco-Vasco[4], Juan Chuquin-Vasco[5], Sebastian Guerrero-Luzuriaga[2]

[1] Escuela Superior Politécnica de Chimborazo (ESPOCH), Environmental Engineering Career, 060101 Riobamba, Ecuador
[2] NotiConsul Consultoria Agroindustrial, 060104 Riobamba, Ecuador
[3] Escuela Superior Politécnica de Chimborazo (ESPOCH), Mechanical Engineering Career, 060101 Riobamba, Ecuador
[4] Escuela Superior Politécnica de Chimborazo (ESPOCH), BI-Data Research Group, 060101 Riobamba, Ecuador
[5] Escuela Superior Politécnica de Chimborazo (ESPOCH), Mining Career, Environment and Engineering Research Group (GISAI); 060101 Riobamba, Ecuador

*** Correspondence:** Email: cristina.calderont@espoch.edu.ec; Tel: 593998724006.

Abstract: Ecuador is a developing country that relies on mining as a significant source of economic income every year; however, there needs to be more studies on the soil pollution caused by mining over time. Biological remediation as an alternative to the use of physical and chemical methods offers a more cost-effective and environmentally friendly means to counteract the negative impacts that the presence of heavy metals in mining tailings soils can cause. This study focused on soil sampling from the mining tailings of the San Carlos de las Minas sector, in the Zamora Chinchipe province in Ecuador, to find potential bacterial strains that can degrade two specific contaminants, mercury (Hg) and cyanide (CN^-). For this purpose, 68 soil subsamples were collected. pH, electrical conductivity, moisture, and the concentration of the contaminants were analyzed and measured. The initial concentration of CN^- was 0.14 mg/kg, and of Hg was 88.76 mg/kg. From the soil samples, eight bacterial strains were isolated, characterized at macroscopic and microscopic levels, and identified at the molecular level. The bacteria were then subjected to degradability tests for CN^- and Hg, obtaining interesting results.

The degradation capacity of CN^- stood out for the strains *Micrococcus aloeverae* and *Pseudomonas alcaliphila*, and for the degradation of Hg, the strains *Hydrogenophaga laconesensis* and *Micrococcus aloeverae* were highlighted, achieving degradation percentages of up to 98.80%. These results emphasize the discovery of these bacterial species with potential use in cyanide and mercury remediation processes.

Keywords: bacterial bioremediation; contamination; mine tailings; cyanide; mercury

1. Introduction

As a developing country, Ecuador views metallic mining as a significant economic activity that contributes to job creation and tax revenue [1]. Despite its benefits, concerns arise regarding the environmental damage caused by this expansion. Water resources, soil, and air are the most affected, along with riverbank deforestation and displacement of indigenous communities [2]. Governmental institutions regulate this activity, mandating the creation of mine tailings for waste disposal. However, there needs to be more consistent monitoring to ensure compliance with environmental regulations. Artisanal or illegal mining exacerbates the problem, discharging sediments directly into nearby water bodies and impacting ecosystems and downstream communities [3].

The significant accumulation of sediments in mine tailings, laden with contaminants such as mercury (Hg), cyanide (CN^-), and other heavy metals, constitutes one of the environmental focal points responsible for a significant decline in soil biological activities [4]. Gold (Au) tailings contain large quantities of toxic substances such as Hg and CN^- used in mining operations. Hg is employed in the Au extraction process because pure Au and volatile Hg can be obtained by heating an Au-Hg alloy [5], and it is known that Hg is a hazardous and persistent environmental contaminant causing clinical conditions in humans [6,7]. Hg in an organism is not essential and does not play a vital role in biological processes. Although traces of heavy metals are naturally observed in soils, their excessive accumulation can deteriorate soil quality and damage surface plants [8]. Furthermore, the absorption of heavy metals by humans, animals, and plants negatively affects biological chains, leading to ecological safety issues [9]. Cyanide is also used in leaching techniques for Au extraction, posing a potential contaminant affecting plants, agricultural areas, and groundwater, representing a risk to human and animal health [10–12].

On the other hand, these sites represent a high scientific interest due to the complex microbial diversity they harbor. They consist of microorganisms that exhibit metal resistance developed through the moderate evolution of their genetic material, being considered beneficial due to their potential for natural bioremediation [13]. Bioremediation has shown outstanding results in removing various organic contaminants and heavy metals [14]. Compared with traditional physical and chemical methods, microbial remediation offers a practical and environmentally friendly approach, featuring advantages such as high efficiency, low cost, and being eco-friendly [15]. The importance of this research arises from the complexity of studying microorganisms inhabiting contaminated environments due to the need for adequate media and methodology [16]. There are reports of microorganisms found in mine tailings with metabolic capacities to reduce, eliminate, or transform contaminants' concentrations and chemical nature in the sediments [17]. For example, strains such as *Escherichia coli*, *Proteus sp*., *Saccharomyces sp*., and *Desulfobacter sp*. have been reported in soils contaminated with Hg [18–20]. There are reports of alkalophilic bacteria belonging to the genera *Bacillus sp*. and *Pseudomonas sp*., which biodegrade free cyanide and thiocyanate [21,22]. However,

more information on tailings in the Zamora Chinchipe province of Ecuador must be provided. Therefore, this study reveals valuable information about interesting bacterial microorganisms with high potential for the bioremediation of Hg and CN^-. It also reveals bacterial species that have not been reported in other articles for use in bioremediation purposes.

2. Materials and methods

2.1. Sampling site

The soil sampling was carried out in duplicate in September 2022 at the main mine tailings of the private company "Mincampa Minera Campanillas S.A", located in the Amazon region, in the San Carlos de las Minas parish (Zamora Chinchipe, Ecuador) (Latitude: 4°3'28.55"S; Longitude: 78°47'15.55"W) at an altitude between 1705–1720 meters above sea level. A systematic grid sampling approach followed, considering that the tailings had an area of 1000 m^2. The number of samples with statistical significance was calculated, resulting in a total of 68-point sub-samples. Each sub-sample was taken at a depth of 10 cm using a sterile spatula. Subsequently, the sub-samples were homogenized to form a composite sample of 1 kg, which was stored in polyethylene bags and transported to the laboratory in a cooler at 4 ℃ for subsequent analysis [23].

2.2. Soil characterization

The physicochemical characterization of the soil was carried out at the soil laboratory of the Polytechnic School of Chimborazo in Ecuador. In accordance with Book VI Annex 2 of the Ecuadorian Environmental Technical Standard [24], five parameters described in Annex 2 were considered: "Parameters for assessing the initial quality of soil according to its use, mining land use component". The parameters considered were pH, electrical conductivity, moisture content, Hg, and CN^-. pH and electrical conductivity were determined in triplicate by dilution in an aqueous medium and by direct measurement using a Jenway 3510 pH meter and COND 51+ conductivity meter based on Environmental Protection Agency (EPA) 9045D [25] and EPA 9050 [26] standards, respectively.

For CN^- determination, the process began with solid-to-liquid extraction through basic digestion with 50% sodium hydroxide following EPA method 9013A [23]. This was followed by analysis using the Pyridine-Pyrazolone colorimetric method (range 0.002–0.240 mg/L CN) based on the American Public Health Association (APHA) method 4500-CN-E using Hach equipment and reagents [27].

The Hg concentration was measured using solid-to-liquid extraction through acid digestion with 65% nitric acid and 50% hydrogen peroxide, followed by determination via atomic absorption spectrophotometry using hydride generation and cold vapor techniques based on EPA method 7471 [28].

2.3. Isolation and purification of bacterial strains

From the composite soil sample, serial dilutions were prepared on a 10-fold basis ranging from 10^{-1} to 10^{-10}. Each dilution was spread onto nutrient agar Petri dishes, and those dishes containing a viable colony count, ranging from 30 to 300, were selected for the isolation and subsequent purification of strains. For strain isolation, colonies showing morphological differences were selected and streaked onto nutrient agar Petri dishes using the streaking procedure and then incubated for 48 hours at 37 ℃. Subsequently, subculturing was performed until pure cultures were obtained.

2.4. Characterization of bacterial strains

Once the strains were isolated, morphological characterization of the colonies was performed through macroscopic observation, determining the color and shape characteristics of the bacterial colonies. Gram staining is a differential method used to distinguish bacteria based on their cell wall composition and to observe their shape more accurately. To perform the staining, first, a smear is prepared from a pure culture sample to be analyzed, followed by fixing the sample using heat. The staining process involves several steps. First, crystal violet is applied for one minute, and Lugol is added to fix the stain. Next, the decolorizer is added, and finally, the sample is stained with safranin for one minute. Subsequently, the sample is observed under the microscope. According to the staining principle, bacteria that appear pink are Gram-negative due to their higher lipid content in the cell wall. Conversely, bacteria that retain the purple color are Gram-positive, characterized by a higher content of peptidoglycans in their cell wall [29].

Each colony was inoculated by stabbing into test tubes containing 3 mL of SIM medium for motility tests. SIM medium is a multitest medium used to evaluate bacterial motility. Positive motility results are indicated by a cloudy area extending away from the inoculation line, while a negative test is characterized by growth only along the inoculation line and no further [30].

Eight bacterial strains were selected for molecular characterization, labeled numerically from 1 to 8. The process began with DNA extraction, followed by evaluation of its quality and integrity through microvolume spectrophotometry and visualization on agarose gel. PCR amplification of the 16S and rpoB fragments was performed using the rpoB primers: rpoB-F/rpoB-R (5'-ATC GAA ACG CCT GAA GGT CCA AAC AT-3'/ 5'-ACA CCC TTG TTA CCG TGA CGA CC-3') [31] for sample 3; and for the other samples, universal 16s primers were used: 27F/1492R (5'-AGAGTTTGATCCTGGCTCAG-3'/5'-GGTTACCTTGTTACGACTT-3') [32]. Once the DNA fragments were amplified, sequencing was performed using Sanger and high throughput methods, followed by assembly using bioinformatics tools. For species identification, DNA sequences were entered into the NCBI Blast platform, and the taxonomy of each strain was determined based on the percentage similarity with the existing database.

2.5. Degradability tests of CN^- *and* Hg

Once the strains were identified at the molecular level, they were subjected to CN^- and Hg degradability tests. These tests were conducted in test tubes containing 10 mL of nutrient broth enriched with sodium cyanide and mercury chloride, respectively. The tests were performed in triplicate at three different concentrations, as shown in Table 1.

Table 1. Contaminant concentration values for degradability tests.

Contaminant	C1	C2	C3
Cyanide (NaCN)	6.83 mg/L	8.04 mg/L	9.47 mg/L
Mercury ($HgCl_2$)	10 mg/L	88 mg/L	100 mg/L

According to the soil analysis conducted at the mining tailings site, no CN^- contamination was reported. Therefore, to determine the concentrations for the CN^- degradability tests, the permissible

limit established in the Remediation Criteria (maximum permissible values) of Annex 2 of Book VI of the Unified Text of Secondary Legislation of the Ministry Environment of Ecuador for commercial and industrial soil, which is 8.0 mg/kg, was considered [24]. From this value, the concentration was increased by 15% and decreased by 15% to obtain the three concentrations mentioned earlier.

In the initial soil analysis, a high Hg concentration was found, indicating a significant level of contamination that must be considered. Therefore, to establish the concentrations of Hg to be used for the degradability tests, a minimum concentration corresponding to the permissible limit established in the Remediation Criteria (maximum permissible values) of Annex 2 of Book VI of the Unified Text of Secondary Legislation of the Ministry Environment of Ecuador for commercial and industrial use, which is 10.0 mg/kg, was used [24]. The second concentration used was based on the mean of the values obtained in the initial physicochemical analysis of the samples, which was 87.575 mg/kg. The maximum concentration corresponds to the value increased by 15% of the annex's permissible limit of 100.7 mg/kg. The bacterial strains were then inoculated into each tube along with the previously established concentrations of CN^- and Hg. The tubes were incubated for five days at 37 ℃, and the Hg and CN^- concentrations were measured at the end of the experiment using the same protocol described in the soil characterization section, Section 2.2. Additionally, the achieved cell density was measured using spectrophotometry with an absorbance of 600 nm. The absorbance of the McFarland standards was then measured to obtain the calibration curve and the mathematical expression correlating absorbance with the number of cells to determine the value of CFU/mL.

2.6. Statistical analysis

The experimental analysis considered the degradation percentage of two contaminants (dependent variable) by eight bacteria isolated from mining tailings soil (independent variable) to assess the ability of each type of bacteria to degrade CN^- and Hg and compare their efficacy. A statistical summary was performed with the obtained data to test for significant differences among the means of the three applied contaminant concentrations. A multiple-range test was conducted to determine if degradation rates are statistically different using STATGRAPHICS 19.0 software.

3. Results and discussion

3.1. Soil characterization

According to the soil characterization in Table 2, an average pH value of 6.14 was obtained, classified as slightly acidic, consistent with the findings of Gürtekin and Aydar [33], which indicate that mine tailings are moderately acidic due to acid drainage caused by the metamorphism and leaching of sulfide-rich minerals, such as reactive pyrite mineral. These values are a consequence of the atmospheric oxidation of exposed pyrite minerals in the tailings deposit, producing sulfuric acid (mine acid drainage) [34,35]. On the other hand, it is expected to find electrical conductivity (EC) values greater than 1500 µS/cm in tailings soils sampled at depths shallower than 60 cm [34,36]. The increase in EC and acidic pH indicate oxidative activity due to the higher presence of oxygen on the surface, microbial activity, and constant water contact [34,37]. It is important to note that, until the development of the present study, a detailed analysis of soil characterization in the parish of Zamora Chinchipe, Ecuador, has not been published, making it difficult to compare the pH and conductivity values observed in Table 2.

Table 2. pH and electrical conductivity values of soil samples from the mining tailings.

Sample	pH	Electrical conductivity, EC (μS/cm)
1	6.23 ± 0.101	1788.51 ± 15.15
2	6.04 ± 0.138	2159.08 ± 4.724
Mean	6.14	1973.80

Hg contamination in artisanal and small-scale gold mining (ASGM) communities is widespread globally. In the process of extracting residual gold after amalgamation, it is often reprocessed with CN^- [38]. For this reason, it was essential to determine the CN^- concentration in the mining tailings soil. The CN^- concentration obtained was 8.0 mg/kg, as shown in Table 3, which is below the permissible limits set by Ecuadorian legislation. However, the detected concentration possibly results from the geological characteristics of the sediment, as leachate waste contains CN^- residues that undergo various changes such as atmospheric dispersion, chemical transformation into other carbon and nitrogen species, and retention in solid form as cyanometallic precipitates or adsorbed species with metals such as cyanate (CNO^-) and thiocyanate (SCN^-) [21,39]. Even Hg reacts with CN^- under aerobic conditions to produce $Hg(CN)_4^{2-}$ and other complexes [38].

Table 3. Physicochemical parameters for initial soil quality analysis.

Sample	Cyanide (CN^-) (mg/kg)	Mercury (Hg) (mg/kg)
1	0.14	75.7
2	0.14	99.45
Mean	0.14	88.75
Permissible limit value *	8.0	10.0

*Note: Annex 2: Remediation Criteria for Contaminated Soils, from the Environmental Quality Standard for Soil Resources and Remediation Criteria for Contaminated Soils in Ecuador.

These analyses are consistent with the study by Zhang et al., which mentions that gold mine tailings have caused severe contamination by heavy metals in soil and water, emphasizing the importance of studying soil quality and its potential impact [40]. However, in Ecuador, there have been no reports of studies on CN^- and Hg mining contamination in the San Carlos parish, but CN^- contamination has been studied in a river in the Portovelo-Zaruma area, with CN^- contamination found even 50 km away from the mines [41,42].

In small-scale hard rock gold mines, some of the particles forming the amalgam with Hg are recovered with gold, while others remain with Hg in the tailings, causing soil contamination [43]. The type of soil clay has impermeable properties where the surface layer retains water until saturated, causing Hg to concentrate and become trapped in the surface layer [44]. Therefore, we were interested in determining the Hg concentration in soil samples, resulting in an average of 88.75 mg/kg, which is lower compared to other soils considered contaminated by Hg, for example, where values of up to 383.21 mg/kg are recorded in Kulon Progo [45]. Studies in Ecuador are scarce, but in 2003, Ram ŕez et al. studied the Hg concentration in mining soils in Nambija and its surroundings (an area

close to our study), showing Hg values of 0.6 to 0.8 mg/kg in soil samples from San Carlos, indicating a significant increase in contamination nine years later [46]. Additionally, this value is eight times higher than the permissible limit under Ecuadorian standards [24]. It deserves attention to seek alternatives to mitigate contamination, as indicated by Romero et al., regarding the importance of developing contamination mitigation strategies and preventing it from reaching crops and continuing to affect human health and the ecosystem in general [47].

3.2. Isolation of bacterial strains

Several physicochemical methods have been employed to decontaminate and recover environments contaminated with heavy metals, such as adsorption, chemical precipitation, nanomaterials, and osmosis. However, their application is limited from both environmental and economic perspectives. For this reason, biotechnology has been explored to develop cost-effective and environmentally friendly processes, such as microbial cells [48] and biosurfactants. These biosurfactants possess a high affinity for heavy metals. Importantly, various microorganisms, including *Pseudomonas sp.*, *Bacillus subtilis*, and *Bacillus sp.*, have been isolated for this purpose, and their success in bioremediation is a testament to the effectiveness of these methods [49].

Once dilutions from 10^{-1} to 10^{-4} were prepared and plated on Petri dishes with nutrient agar, Petri dishes showing viable growth between 30 and 300 colonies were selected. These dishes underwent four cycles of isolation, restreaking, and purification. Ultimately, 15 bacterial strains were obtained, labeled, and morphologically characterized, as described in Table 4.

Table 4. Macroscopic characterization of bacterial strains isolated from soil.

Label	Color	Shape	Edge	Elevation	Texture	Shine
3,–1,1 °,1*	White	Irregular	Lobed	Flat	Rough	Dull
3,–1,8 °,2	Yellow	Circular	Entire	Raised	Smooth	Shiny
3,–2,3 °,1*	Yellow	Circular	Entire	Convex	Smooth	Shiny
3, –9,1 °,1*	White	Irregular	Lobed	Flat	Rough	Dull
4,–1,6 °,1,1*	White	Irregular	Lobed	Flat	Smooth	Shiny
4,–1,6 °,1,2	Yellow	Circular	Entire	Raised	Smooth	Shiny
4,–1,6 °,1,3	White	Irregular	Irregular	Flat	Smooth	Dull
4,–1,6 °,2,1	Yellow	Circular	Entire	Raised	Smooth	Shiny
4,–1,6 °,2,2	Dark yellow	Circular	Entire	Raised	Smooth	Dull
4,–1,6 °,2,3*	Yellow	Circular	Entire	Raised	Smooth	Shiny
4,–1,7 °,1,1*	Dark yellow	Circular	Entire	Convex	Smooth	Dull
4,–2,1 °,2,1*	White	Filamentous	Filamentous	Flat	Rough	Dull
4,–2,1 °,2,2*	Yellow	Circular	Entire	Raised	Smooth	Shiny
4,–2,4 °,1,1	Yellow	Irregular	Rhizoid	Flat	Rough	Shiny
4,–4,1 °,1,1	White	Rhizoid	Rhizoid	Flat	Smooth	Shiny

*Note: Strains chosen for molecular-level identification.

3.3. Characterization of bacterial strains

Eight strains were selected based on their macroscopic characteristics and subjected to Gram staining and mobility tests. Five strains were identified as Gram-positive species, and three strains

were identified as Gram-negative, as observed in Table 5. Regarding shape, both cocci and bacilli types were found. In the mobility tests, five strains yielded positive results, while three strains showed no mobility.

Table 5. Gram staining and bacterial mobility tests.

Bacterial strain	Gram staining	Morphology	Mobility
E1	–	Bacilli	+
E2	–	Cocci	+
E3	+	Bacilli	+
E4	+	Bacilli	–
E5	+	Staphylococci	–
E6	+	Cocci	–
E7	+	Bacilli	+
E8	–	Coccobacilli	+

*Note: *+: Gram positive; –: Gram negative; +: Positive mobility; –: Negative mobility.*

The DNA obtained from sample E1 was sent for high-throughput sequencing after amplicon library preparation, while the other DNA samples (E2 to E8) were sequenced using the Sanger method. Subsequently, molecular identification was performed by comparing the DNA sequences obtained with the GenBank nucleotide database from NCBI for bacterial identification, and the results are shown in Table 6.

Table 6. Molecular identification.

Original code	Fragment length (bp)	% Fragment quality	Organism	Fragment	% Species identity	Accession Number
E1	1459	…	*Pseudomonas chengduensis*	16S	100	NR 125523.1
E2	168	89.8	*Pseudomonas alcaliphila*	16S	98.8	NR 114072.1
E3	1035	99.8	*Bacillus subtilis*	rpoB	100	CP053102.1
E4	147	94.6	*Bacillus altitudinis*	16S	99.32	MT569984.1
E5	762	100	*Staphylococcus saprophyticus*	16S	100	CP035294.1
E6	768	99.7	*Micrococcus aloeverae*	16S	100	NR 134088.1
E7	683	99.9	*Bacillus subtilis*	16S	99.71	OP986262.1
E8	749	99.7	*Hydrogenophaga laconesensis*	16S	99.6	NR 149183.1

3.4. CN^- and mercury Hg degradability tests

The McFarland scale standards were used; their absorbance at 600 nm was measured, and this variable was correlated with the number of cells measured in CFU/mL representing each standard. An equation was obtained to express this relationship. The equation is described as: $y = 17{,}394x - 0{,}966$; where *y* is the number of cells and *x* is the absorbance measured in each sample shown in Table 7.

Table 7. McFarland scale.

McFarland Standard Number	Volume $BaCl_2$ 1% (mL)	Volume H_2SO_4 1% (mL)	Number of cells ($1x10^8$ CFU/mL)	Absorbance at 600nm
0.5	0.05	9.95	1.5	0.097
1	0.1	9.90	3	0.236
2	0.2	9.80	6	0.422
3	0.3	9.70	9	0.584
4	0.4	9.60	12	0.745
5	0.5	9.50	15	0.934
6	0.6	9.40	18	1.106
7	0.7	9.30	21	1.272
8	0.8	9.20	24	1.424
9	0.9	9.10	27	1.588
10	1.0	9.00	30	1.775

In the cyanide medium, a maximum cell density of $2.41x10^8$ CFU/mL was recorded, reached by the species *Hydrogenophaga laconesensis*. Following this, *Bacillus altitudinis* and *Pseudomonas alcaliphila* exhibited average densities of $1.84x10^8$ CFU/mL and $1.65x10^8$ CFU/mL, respectively. For *Micrococcus aloeverae* and *Staphylococcus saprophyticus*, cell densities of up to $1.5x10^8$ CFU/mL and $1.37x10^8$ CFU/mL were reached, respectively. The species with the most minor cell development were *Pseudomonas chengduensis* and *Bacillus subtilis*, with averages of $1.06x10^8$ CFU/mL and $0.72x10^8$ CFU/mL, respectively. It is worth noting that the species E7 (*Bacillus subtilis*) achieved superior development, with $1.46x10^8$ CFU/mL, compared to E3 (*Bacillus subtilis*), despite being the same species. The averages reached by each species at their three concentrations are detailed in Table 8 below:

Table 8. Cell density in the cyanide and mercury medium.

Bacterial strain	Concentration	Cyanide medium		Mercury medium	
		Absorbance	Number of cells ($1x10^8$ CFU/mL)	Absorbance	Number of cells ($1x10^8$ CFU/mL)
E1	C1	0.062	0.954	0.181	2.182
	C2	0.065	1.010	0.162	1.846
	C3	0.079	1.216	0.188	2.304
E2	C1	0.100	1.552	0.259	3.533
	C2	0.133	2.057	0.180	2.159
	C3	0.087	1.340	0.153	1.689
E3	C1	0.044	0.675	0.073	1.124
	C2	0.044	0.680	0.079	1.227
	C3	0.051	0.794	0.080	1.232
E4	C1	0.122	1.881	0.128	1.255
	C2	0.103	1.588	0.162	1.858
	C3	0.133	2.052	0.157	1.771
E5	C1	0.096	1.485	0.070	1.077
	C2	0.091	1.402	0.130	1.289
	C3	0.079	1.216	0.116	1.046
E6	C1	0.072	1.108	0.190	2.345
	C2	0.101	1.557	0.203	2.571
	C3	0.119	1.835	0.142	1.504
E7	C1	0.107	1.655	0.104	0.837
	C2	0.083	1.278	0.115	1.034
	C3	0.093	1.443	0.100	0.779
E8	C1	0.136	2.108	0.140	1.475
	C2	0.154	2.387	0.161	1.834
	C3	0.146	2.253	0.187	2.281

On the other hand, in the medium with Hg, bacterial strains exhibited higher cell growth, reaching maximum values of $3.53x10^8$ CFU/mL, with species such as *Pseudomonas alcaliphila*, *Micrococcus aloeverae,* and *Hydrogenophaga laconesensis* showing the highest cell densities. Species with lower growth were E3 and E7, corresponding to *Bacillus subtilis* and *Staphylococcus saprophyticus*, with cell densities between $0.78x10^8$ CFU/mL and $1.29x10^8$ CFU/mL. These obtained values may indicate more excellent resistance to Hg compared to cyanide CN^-. These results could be attributed to bacteria adapting to high Hg concentrations and naturally developing resistance even to higher contaminant levels. It is essential to mention that the bacterial genera, *Bacillus* and *Pseudomonas*, have been extensively reported in investigations to reduce other contaminants, such as Cr (VI). These studies have documented reductions from 80 to 30 mg/L, highlighting the significance of these genera in bioremediation processes of environments contaminated with heavy metals [50].

Despite the toxicity of CN^-, it is a compound that can be synthesized by various organisms, including bacteria, fungi, plants, or animals, employing cyanogenesis as a survival mechanism in contaminated environments [51]. Several organisms have developed metabolic pathways for CN^-

degradation, transformation, assimilation, or tolerance and can even use it as the sole nitrogen source for growth [52]. Microorganisms utilize degradative pathways involving enzymes in hydrolytic, oxidative, reductive, and substitution-transfer reactions for CN^- degradation [22,53,54].

The CN^- degradability tests generally determined that bacterial strains achieved degradation percentages between 7.94% and 66.24%. It was noted that this percentage was lower at concentration C1, reaching a maximum value of 36.51%, and significantly increased for concentrations C2 and C3, with the latter registering the highest CN^- degradation values, as shown in Figure 1.

Some interesting results were also found due to the action of *Micrococcus aloeverae*, reaching the highest degradation value (66.24%). This bacterium has been reported in studies on wastewater treatment [55] and pesticide degradation [56] but not specifically in CN^- removal. The species *Pseudomonas alcaliphila* recorded a maximum degradation percentage of 64.76%. While this bacterium has been reported in processes such as biodegradation of Ni-citrate complexes, Ni (Nickel) recovery [57], and copper bioremediation [58], its activity against CN^- or Hg has not been reported. However, these activities suggest that *Pseudomonas sp*. may have the potential for cyanide or mercury degradation [22]. Finally, the species *Bacillus subtilis* reported a degradation percentage of 60.30%, which is consistent with previous findings [59]. These degradation percentages were achieved at the maximum concentration of C3, as shown in Figure 1.

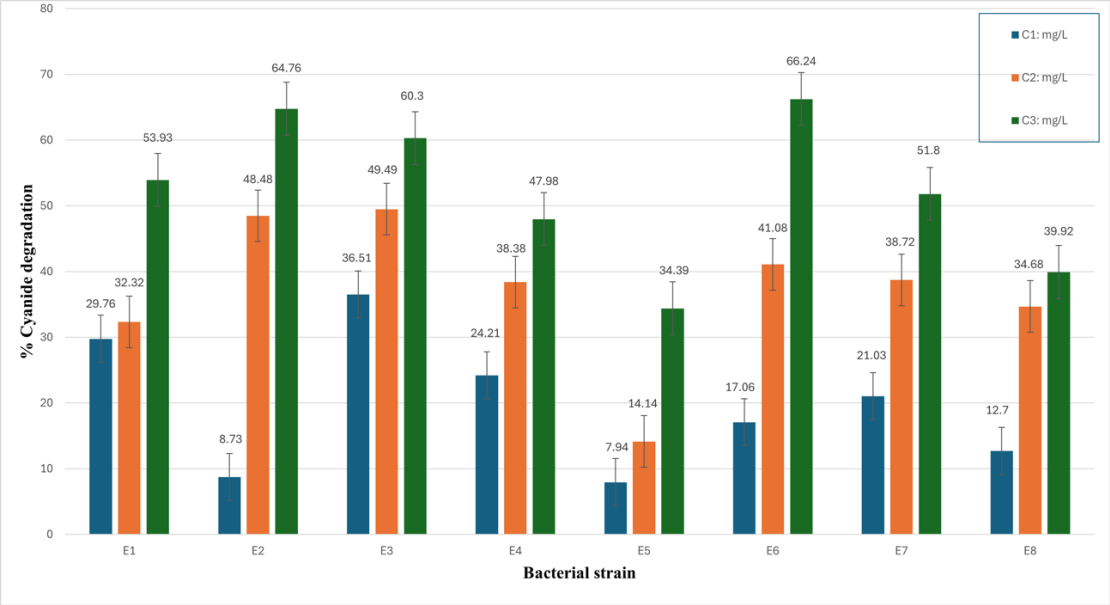

Figure 1. Percentage of cyanide (CN^-) degradation for bacterial strains labeled from E1 to E8. Initial contaminant concentrations: C1 (6.83 mg/L), C2 (8.04 mg/L), C3 (9.47 mg/L). Bacterial species corresponding to the label: E1 (*Pseudomonas chengduensis*), E2 (*Pseudomonas alcaliphila*), E3 (*Bacillus subtilis*), E4 (*Bacillus altitudinis*), E5 (*Staphylococcus saprophyticus*), E6 (*Micrococcus aloeverae*), E7 (*Bacillus subtilis*), E8 (*Hydrogenophaga laconesensis*). Error bars indicate a standard deviation from the mean activities of triplicate assays.

When analyzing the degradability of CN^- at three different initial concentrations, we focused on the coefficient of variation shown in Table 9. The experiment showed that bacteria exposed to concentration C1 exhibited more significant variability in degradation data compared to concentrations C2 and C3, where the bacteria demonstrated more consistent degradation.

Table 9. Summary statistics of cyanide (CN^-) degradation analysis.

	Count	Average	Coeff. of variation
C1 (mg/L)	8	19.742	51.387%
C2 (mg/L)	8	37.161	29.808%
C3 (mg/L)	8	52.415	21.741%
Total	24	36.439	47.063%

A statistical, multiple-range test was conducted to determine if CN^- degradation rates differed statistically, analyzing each concentration separately. This method discriminated among the means using Fisher's least significant difference (LSD) procedure. With this method, there is a 5.0% risk of considering each pair of means as significantly different when the actual difference is equal to 0. According to the results from Table 10, CN^- degradation rates achieved for all bacterial strains used at the initial CN^- concentrations C1 (6.83 mg/L), C2 (8.04 mg/L), and C3 (9.47 mg/L) show no significant differences. This study indicates that bacteria degrade CN^- similarly, regardless of the initial concentration of the contaminant.

Table 10. Multiple-range test. Method: 95.0 percent LSD for the cyanide (CN^-) contaminant.

	Count	Mean	Homogeneous Groups
C1 (mg/L)	8	1.427	A
C1 (mg/L)	8	1.427	A
C2 (mg/L)	8	1.494	A
C3 (mg/L)	8	1.518	A
Contrast	Sig.	Difference	+/– Limits
C1–C2		–0.067	0.512
C1–C3		–0.091	0.512
C1–C1		0	0.512
C2–C3		–0.023	0.512
C2–C1		0.067	0.512
C3–C1		0.091	0.512

The preceding analysis corresponds to Figure 2, which depicts the range in which the maximum cyanide degradation data are concentrated. The data with the least variability are the values with the C3 concentration of the contaminant, which range between 34.39% and 66.2%; however, variability is observed for all three concentrations of the contaminant.

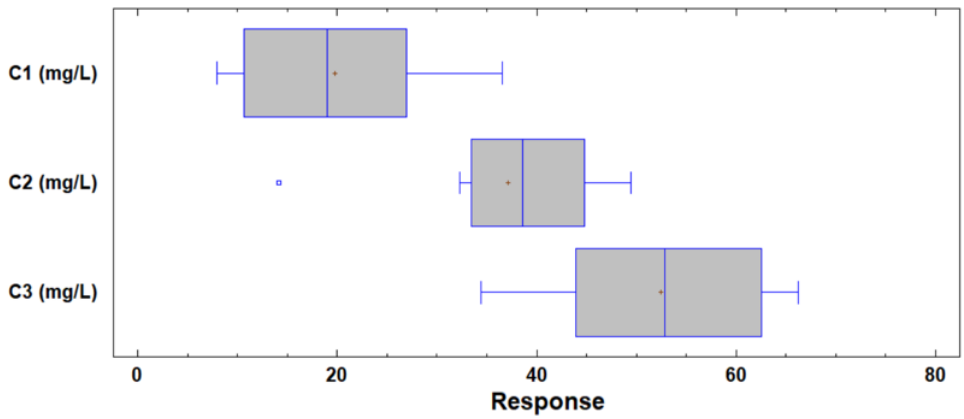

Figure 2. Box plot of CN^- degradability by the eight bacterial strains concerning three different contaminant concentrations: C1 (6.83 mg/L), C2 (8.04 mg/L), C3 (9.47 mg/L).

Studies conducted to date, where the potential of microorganisms for heavy metal degradation, in this case Hg, has been determined, have also allowed the establishment of the characteristics that confer this capacity. Like CN^-, enzymatic pathways that transform, reduce, and/or assimilate mercury have been identified. There is chromosomal level identification data on the genes encoding these functions. An important mechanism of microbial resistance to mercury is its reduction to elemental mercury (facilitated by the *mer*A gene) [60,61]. Other studies establish mercury degradation pathways, primarily mediated by the regulation of the *mer* gene by *mer*R in Gram-negatives and by *mer*R2 in Gram-positives. These are transcription regulatory proteins of the *mer* operon, which have a high affinity for Hg^{2+}, and the *mer*A and *mer*B genes are also mentioned [61–64].

For degradability tests in the mercury medium, percentages greater than 85% were obtained for all species and concentrations evaluated. The species *Hydrogenophaga laconesensis* achieved the highest percentages, ranging from 99.44% to 99.80%, for all three concentrations. This species has been reported for potential use in oil bioremediation [65], but based on these findings, it can also be used in Hg removal. Additionally, *Pseudomonas alcaliphila* and *Micrococcus aloeverae* showed degradation rates of 98.97% and 98.78%, respectively. There are not many studies on *Micrococcus aloeverae* in the area of heavy metal bioremediation, but it is clear that it is a potential candidate for these processes as indicated by the study of Pandit et al. [66].

The three species showed similar degradation percentages across the three concentrations, while the remaining species did not exceed 89% at concentration C1. This result is likely due to lower cell densities at this concentration, resulting in decreased contaminant degradation due to the reduced number of cells present. On the other hand, for concentrations C2 and C3, percentages between 96.28% and 99.07% were achieved. Finally, the species with the lowest performance was strain E5, which degraded 66.91% of the Hg in the sample at its initial concentration but achieved good degradation values (96.72% and 96.41%) for concentrations C2 and C3. Figure 3 provides detailed descriptions of the degradation percentages in the mercury medium achieved by each species at their three test concentrations. These findings underscore the crucial component of the remediation process: Studying the microbial population in a contaminated environment. Advanced technical approaches are needed to understand the dynamic aspects of microbial activity and survival in a stressed environment [67].

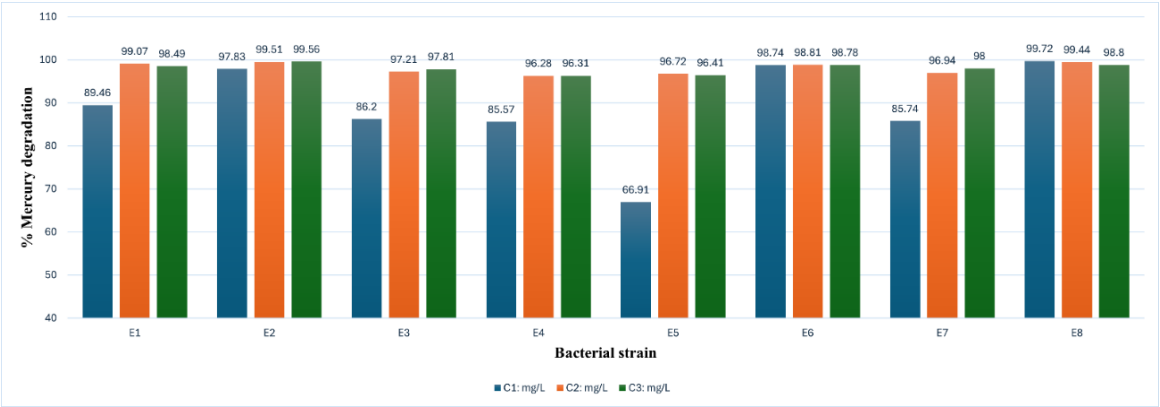

Figure 3. Percentage of mercury (Hg) degradation for bacterial strains labeled from E1 to E8. Initial contaminant concentrations: C1 (10 mg/L), C2 (88 mg/L), C3 (100 mg/L). Bacterial species corresponding to the label: E1 (*Pseudomonas chengduensis*), E2 (*Pseudomonas alcaliphila*), E3 (*Bacillus subtilis*), E4 (*Bacillus altitudinis*), E5 (*Staphylococcus saprophyticus*), E6 (*Micrococcus aloeverae*), E7 (*Bacillus subtilis*), E8 (*Hydrogenophaga laconesensis*).

When analyzing the degradability of mercury at three different initial concentrations, we focused on the coefficient of variation shown in Table 11. The coefficient of variation allows us to assess the relative variability of the data. In the experiment, it was observed that bacteria exposed to concentration C1 of the contaminant exhibited more significant variability in degradation data compared to concentrations C2 and C3, which showed lower variability. This study demonstrates that bacteria exposed to higher Hg contaminant concentrations generate more consistent degradation.

Table 11. Summary statistics of Hg degradation analysis.

	Count	Average	Coeff. of variation
C1 (mg/L)	8	88.77	12.09%
C2 (mg/L)	8	97.99	1.36%
C3 (mg/L)	8	98.02	1.18%
Total	24	94.93	7.87%

Based on the previous statistical results in Table 11, a multiple-range test was conducted to determine if the degradation rates of the contaminant Hg were statistically different. According to the results in Table 12, the mercury degradation rates achieved for all bacterial strains used at an initial mercury concentration of 88 mg/L (C2) and 100 mg/L (C3) were similar. However, both significantly differ from the mercury concentration of 10 mg/L (C1). As observed, it is confirmed that bacteria degrade more effectively when exposed to a culture medium with high mercury concentrations (C2 and C3), and their degradation level decreases when they grow in a culture medium with low mercury concentrations. This information is essential for determining the optimal starting concentration of the contaminant at which these bacteria can work in bioremediation processes.

Table 12. Multiple-range test. Method: 95.0 percent LSD for the mercury (Hg) contaminant.

	Count	Mean	Homogeneous Groups
C1 (mg/L)	8	88.7713	A
C2 (mg/L)	8	97.9975	B
C3 (mg/L)	8	98.02	B
Contrast	Sig.	Difference	+/– Limits
C1–C2	*	–9.2262	6.52756
C1–C3	*	–9.24875	6.52756
C2–C3		–0.0225	6.52756

This analysis corresponds to Figure 4, which displays the range where the maximum Hg degradation data concentrate for concentrations C2 and C3. These values range between 96.28% and 99.56%, unlike concentration C1, where most of the degradation concentrates within the 86% to 98% range, with an outlier value of 66.91% degradation. Therefore, it is concluded that, regardless of the contaminant (Hg or CN^-), bacteria respond better to degradation when grown in media with higher contaminant concentrations.

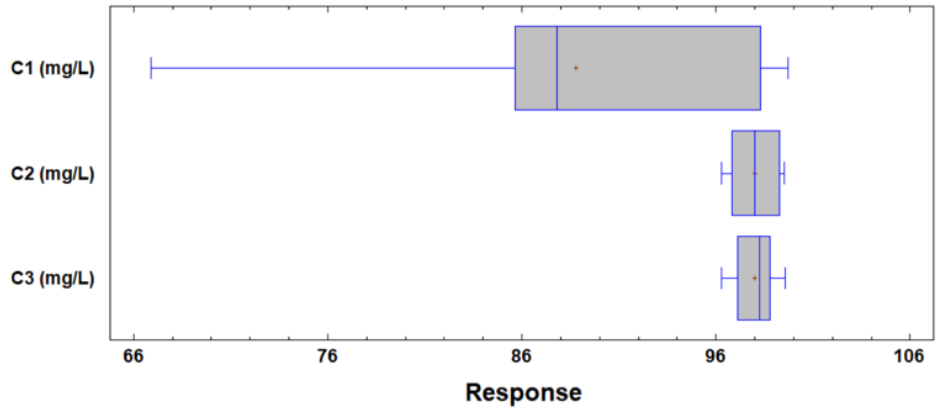

Figure 4. Box plot of Hg degradability by the eight bacterial strains concerning three different contaminant concentrations: 10 mg/L (C1), 88 mg/L (C2), and 100 mg/L (C3).

5. Conclusions

This study focused on isolating 15 bacterial strains from soil samples from mining tailings in the San Carlos area of Ecuador. Molecular identification revealed 5 genera, including *Pseudomonas*, *Bacillus*, *Staphylococcus*, *Micrococcus*, and *Hydrogenophaga*. The degrading potential of these strains against three different concentrations of CN^- and Hg was evaluated in the laboratory. For CN^-, concentrations of 6.8 mg/L, 8 mg/L, and 9.2 mg/L were used, while for Hg, concentrations of 10 mg/L, 88 mg/L, and 100 mg/L were employed. It was observed that bacteria exhibit superior degradation performance when grown in media with higher contaminant concentrations compared to lower concentrations.

CN^- degradation ranged from 7.94% to 66.24%, with *Micrococcus aloeverae* and *Pseudomonas alcaliphila* showing the highest rates. These strains, not previously mentioned in cyanide degradation studies, are promising for CN^- removal processes. *Bacillus subtilis* also showed satisfactory results, reaffirming its known effectiveness. For Hg degradation, bacterial strains achieved over 85% efficacy

at the lowest concentration (10 mg/L). Higher concentrations led to even better removal rates, reaching 96.31% to 98.80% at 88 mg/L and 100 mg/L, respectively. Notable Hg degraders included *Hydrogenophaga laconesensis* and *Micrococcus aloeverae*, which were previously unidentified. *Pseudomonas alcaliphila* effectively degraded both Hg and CN^-. The study suggests further exploration and application of these bacteria from contaminated mining tailings in forming bacterial consortia, highlighting their significant potential in bioremediation processes to mitigate environmental pollution.

Use of AI tools declaration

The authors declare that artificial intelligence (AI) tools were not used in any stage of research in the studies carried out and presented in this article.

Acknowledgments

The authors would like to express their utmost gratitude to all parties who have contributed to the successful implementation of this research.

Conflicts of interest

The authors declare no conflict of interest.

References

1. Betancourt O, Narv áez A, Roulet M (2005) Small-scale gold mining in the Puyango River basin, southern Ecuador: A study of environmental impacts and human exposures. *Ecohealth* 2: 323–332. https://doi.org/10.1007/s10393-005-8462-4
2. Counter SA, Buchanan LH, Ortega F, et al. (2002) Elevated blood mercury and neuro-otological observations in children of the Ecuadorian gold mines. *J Toxicol Env Heal A* 65: 149–163. https://doi.org/10.1080/152873902753396785
3. Conde M (2017) Resistance to mining. A Review. *Ecol Econ* 132: 80–90. https://doi.org/10.1016/j.ecolecon.2016.08.025
4. Hedrick DB, Peacock A, Stephen JR, et al. (2000) Measuring soil microbial community diversity using polar lipid fatty acid and denaturing gradient gel electrophoresis data. *J Microbiol Meth* 41: 235–248. https://doi.org/10.1016/S0167-7012(00)00157-3
5. Chamba I, Rosado D, Kalinhoff C, et al. (2017) Erato polymnioides–A novel Hg hyperaccumulator plant in ecuadorian rainforest acid soils with potential of microbe-associated phytoremediation. *Chemosphere* 188: 633–641. https://doi.org/10.1016/j.chemosphere.2017.08.160
6. Jing X, Lu T, Sun F, et al. (2023) Microbial transformation to remediate mercury pollution: Strains isolation and laboratory study. *Int J Environ Sci Te* 20: 3039–3048. https://doi.org/10.1007/s13762-022-04158-z
7. Kannan SK, Mahadevan S, Krishnamoorthy R (2006) Characterization of a mercury-reducing Bacillus cereus strain isolated from the Pulicat Lake sediments, south east coast of India. *Arch Microbiol* 185: 202–211. https://doi.org/10.1007/s00203-006-0088-6
8. Deng S, Zhang X, Zhu Y, et al. (2024) Recent advances in phyto-combined remediation of heavy metal pollution in soil. *Biotechnol Adv* 72. https://doi.org/10.1016/j.biotechadv.2024.108337

9. Chen L, Zhang X, Zhang M, et al. (2022) Removal of heavy-metal pollutants by white rot fungi: Mechanisms, achievements, and perspectives. *J Clean Prod* 354. https://doi.org/10.1016/j.jclepro.2022.131681
10. Purchase MDW, Castillo J, Arias AG, et al. (2024) First insight into the natural biodegradation of cyanide in a gold tailings environment enriched in cyanide compounds. *Sci Total Environ* 906: 167174. https://doi.org/10.1016/j.scitotenv.2023.167174
11. Jabbar KA, Akhter G, Gabriel HF, et al. (2020) Anthropogenic effects of coal mining on ecological resources of the Central Indus basin, Pakistan. *Int J Env Res Pub He* 17: 1255. https://doi.org/10.3390/ijerph17041255
12. Boerleider RZ, Roeleveld N, Scheepers PTJ (2017) Human biological monitoring of mercury for exposure assessment. *AIMS Environ Sci* 4: 251–276. https://doi.org/10.3934/environsci.2017.2.251
13. Torsvik V, Øvreås L (2002) Microbial diversity and function in soil: from genes to ecosystems. *Curr Opin Microbiol* 5: 240–245. https://doi.org/10.1016/S1369-5274(02)00324-7
14. Gao X, Wei M, Zhang X, et al. (2024) Copper removal from aqueous solutions by white rot fungus Pleurotus ostreatus GEMB-PO1 and its potential in co-remediation of copper and organic pollutants. *Bioresource Technol* 395. https://doi.org/10.1016/j.biortech.2024.130337
15. Cao S, Duan M, Zhang X, et al. (2024) Bacterial community structure analysis of sludge from Taozi Lake and isolation of an efficient 17β-Estradiol (E2) degrading strain Sphingobacterium sp. GEMB-CSS-01. *Chemosphere* 355: 141806. https://doi.org/10.1016/j.chemosphere.2024.141806
16. Narayanan M, Devarajan N, He Z, et al. (2020) Assessment of microbial diversity and enumeration of metal tolerant autochthonous bacteria from tailings of magnesite and bauxite mines. *Mater Today Proc* 33: 4391–4401. https://doi.org/10.1016/j.matpr.2020.07.652
17. Mungla G, Facknath S, Lalljee B (2022) Assessing the potential of mechanical aeration combined with bioremediation process in soils and coastal sediments impacted by heavy metals. *AIMS Environ Sci* 9: 692–707. https://doi.org/10.3934/environsci.2022039
18. Chen SC, Lin WH, Chien CC, et al. (2018) Development of a two-stage biotransformation system for mercury-contaminated soil remediation. *Chemosphere* 200: 266–273. https://doi.org/10.1016/j.chemosphere.2018.02.085
19. Rodríguez MB, Piedra CAJ, Chiocchetti GDME, et al. (2016) The use of Saccharomyces cerevisiae for reducing mercury bioaccessibility. *Toxicol Lett* 258: S159. https://doi.org/10.1016/j.toxlet.2016.06.1604
20. Ignatavičius G, Unsal MH, Busher PE, et al. (2022) Geochemistry of mercury in soils and water sediments. *AIMS Environ Sci* 9: 261–281. https://doi.org/10.3934/environsci.2022019
21. Rivera AA, Hoyos SG, Buitrón G, et al. (2021) Biological treatment for the degradation of cyanide: A review. *J Mater Res Technol* 12: 1418–1433. https://doi.org/10.1016/j.jmrt.2021.03.030
22. Almagro VML, Huertas MJ, Luque MM, et al. (2005) Bacterial degradation of cyanide and its metal complexes under alkaline conditions. *Appl Environ Microb* 71: 940–947. https://doi.org/10.1128/AEM.71.2.940-947.2005
23. Standard Practices for Preserving and Transporting Soil Samples, ASTM International (2009) Ingeniería Civil en el Slavador. ASTM Designation D 4220-00, 2009. Available from: https://worldwidestandard.net/wp-content/uploads/2019/07/D-4220.pdf.
24. Ministerio del Ambiente Ecuador (2015) Edición Especial Nº 387-Registro Oficial. 387: 17–18.
25. EPA (2004) Method 9045D-soil and waste pH, EPA D.pdf, 2004. Available from: https://www.epa.gov/sites/default/files/2015-12/documents/9045d.pdf.

26. EPA (1996) Method 9050A specific conductance, EPA, 1996. Available from: https://www.epa.gov/sites/default/files/2015-12/documents/9050a.pdf.
27. American public health association (1997) By Authority Of. Available from: https://law.resource.org/pub/us/cfr/ibr/002/apha.method.4500-cn.1992.pdf.
28. Yalkowsky S, He Y, Jain P (2010) Chemical abstracts service registry number (RN), *Handbook of Aqueous Solubility Data*, 2Eds., CRC Press, 1575–1608. https://doi.org/10.1201/EBK1439802458-6
29. Tantray JA, Mansoor S, Wani RFC, et al. (2023) Gram staining of bacteria, *Basic Life Sci Methods*. https://doi.org/10.1016/B978-0-443-19174-9.00043-X
30. Shields P, Cathcart L (2016) Motility test medium protocol. *Am Soc Microbiol* 214: 215.
31. Ki JS, Zhang W, Qian PY (2009) Discovery of marine bacillus species by 16S rRNA and rpoB comparisons and their usefulness for species identification. *J Microbiol Meth* 77: 48–57. https://doi.org/10.1016/j.mimet.2009.01.003
32. Polo CPL, Lebonguy AA, Boumba AEL, et al. (2022) Bacterial community diversity of a Congolese traditional fermented food, "Pandé", revealed by Illumina Miseq^{TM} Sequencing of 16S rRNA Gene. *Open J Appl Sci* 12: 387–405. https://doi.org/10.4236/ojapps.2022.123027
33. Gürtekin G, Aydar E (2023) Quantitative Mineralogy in characterization of historical tailings: A case from the abandoned Balya Pb-Zn mine, Western Turkey. *Nat Resour Res* 32: 195–212. https://doi.org/10.1007/s11053-022-10128-6
34. Dinis ML, Fiúza A, Futuro A, et al. (2020) Characterization of a mine legacy site: an approach for environmental management and metals recovery. *Environ Sci Pollut R* 27: 10103–10114. https://doi.org/10.1007/s11356-019-06987-x
35. Kagambega N, Sam U, Ouedraogo M (2023) Artisanal mining and soil quality in the Sudano-Sahelian climate: Case of the artisanal mining site of Yimiougou in Burkina Faso, West Africa. *J Environ Prot* 14: 1–15. https://doi.org/10.4236/jep.2023.141001
36. Esshaimi M, EI Gharmali A, Berkhis F, et al. (2017) Speciation of heavy metals in the soil and the mining residues, in the zinclead Sidi Bou Othmane abandoned mine in Marrakech area. *Linnaeus Eco-Tech* 975–985. https://doi.org/10.15626/Eco-Tech.2010.102
37. Nkongolo KK, Spiers G, Beckett P, et al. (2022) Inside old reclaimed mine tailings in Northern Ontario, Canada: A microbial perspective. *Ecol Genet Genomics* 23: 100118. https://doi.org/10.1016/j.egg.2022.100118
38. Seney CS, Bridges CC, Aljic S, et al. (2020) Reaction of cyanide with Hg 0-contaminated gold mining tailings produces soluble mercuric cyanide complexes. *Chem Res Toxicol* 33: 2834–2844. https://doi.org/10.1021/acs.chemrestox.0c00211
39. Johnson CA (2015) The fate of cyanide in leach wastes at gold mines: An environmental perspective. *Appl Geochem* 57: 194–205. https://doi.org/10.1016/j.apgeochem.2014.05.023
40. Zhang C, Wang X, Jiang S, et al. (2021) Heavy metal pollution caused by cyanide gold leaching: A case study of gold tailings in central China. *Environ Sci Pollut R* 28: 29231–29240. https://doi.org/10.1007/s11356-021-12728-w
41. Marshall BG, Veiga MM, da Silva HAM, et al. (2020) Cyanide contamination of the Puyango-Tumbes River caused by artisanal gold mining in Portovelo-Zaruma, Ecuador. *Curr Env Hlth Rep* 7: 303–310. https://doi.org/10.1007/s40572-020-00276-3
42. Miserendino RA, Bergquist BA, Adler SE, et al. (2013) Challenges to measuring, monitoring, and addressing the cumulative impacts of artisanal and small-scale gold mining in Ecuador. *Resour Policy* 38: 713–722. https://doi.org/10.1016/j.resourpol.2013.03.007

43. Yoon S, Kim DM, Yu S, et al. (2023) Metal(loid)-specific sources and distribution mechanisms of riverside soil contamination near an abandoned gold mine in Mongolia. *J Hazard Mater* 443: 130294. https://doi.org/10.1016/j.jhazmat.2022.130294
44. Laker MC, Nortj é GP (2020) Review of existing knowledge on subsurface soil compaction in South Africa. *Adv Agron* 143–197. https://doi.org/10.1016/bs.agron.2020.02.003
45. Rachman RM, Mangidi U, Trihadiningrum Y (2023) Solidification and stabilization of mercury-contaminated tailings in artisanal and small-scale gold mining using tras soil. *J Degr Min Lands Manag* 10: 4575. https://doi.org/10.15243/jdmlm.2023.104.4575
46. Requelme MER, Ramos JFF, Ang élica RS, et al. (2003) Assessment of Hg-contamination in soils and stream sediments in the mineral district of Nambija, Ecuadorian Amazon (example of an impacted area affected by artisanal gold mining). *Appl Geochem* 18: 371–381. https://doi.org/10.1016/S0883-2927(02)00088-4
47. Est évez DR, J ácome GSY, Navarrete H (2023) Non-essential metal contamination in Ecuadorian agricultural production: A critical review. *J Food Compos Anal* 115: 104932. https://doi.org/10.1016/j.jfca.2022.104932
48. Tapia CC, Vasco DC, Galarza AG, et al. (2023) Bioelectricity production from anaerobically treated leachate in microbial fuel cell using Delftia acidovorans spp. *AIMS Environ Sci* 10: 847–867. https://doi.org/10.3934/environsci.2023046
49. Mishra S, Lin Z, Pang S, et al. (2021) Biosurfactant is a powerful tool for the bioremediation of heavy metals from contaminated soils. *J Hazard Mater* 418. https://doi.org/10.1016/j.jhazmat.2021.126253
50. Mishra S, Chen S, Saratale GD, et al. (2021) Reduction of hexavalent chromium by Microbacterium paraoxydans isolated from tannery wastewater and characterization of its reduced products. *J Water Process Eng* 39. https://doi.org/10.1016/j.jwpe.2020.101748
51. Blumer C, Haas D (2000) Mechanism, regulation, and ecological role of bacterial cyanide biosynthesis. *Arch Microbiol* 173: 170–177. https://doi.org/10.1007/s002039900127
52. Park JM, Sewell BT, Benedik MJ (2017) Cyanide bioremediation: The potential of engineered nitrilases. *Appl Microbiol Biot* 101: 3029–3042. https://doi.org/10.1007/s00253-017-8204-x
53. Almagro VML, Cabello P, S áez LP, et al. (2018) Exploring anaerobic environments for cyanide and cyano-derivatives microbial degradation. *Appl Microbiol Biot* 102: 1067–1074. https://doi.org/10.1007/s00253-017-8678-6
54. Mahendran R, Bs S, Thandeeswaran M, et al. (2020) Microbial (Enzymatic) degradation of cyanide to produce pterins as cofactors. *Curr Microbiol* 77: 578–587. https://doi.org/10.1007/s00284-019-01694-9
55. Saim AK, Adu PCO, Amankwah RK, et al. (2021) Review of catalytic activities of biosynthesized metallic nanoparticles in wastewater treatment. *Environ Technol Rev* 10: 111–130. https://doi.org/10.1080/21622515.2021.1893831
56. Chandrasekaran M, Paramasivan M (2024) Plant growth-promoting bacterial (PGPB) mediated degradation of hazardous pesticides: A review. *Int Biodeter Biodegr* 190: 105769. https://doi.org/10.1016/j.ibiod.2024.105769
57. Qian J, Li D, Zhan G, et al. (2012) Simultaneous biodegradation of Ni-citrate complexes and removal of nickel from solutions by Pseudomonas alcaliphila. *Bioresource Technol* 116: 66–73. https://doi.org/10.1016/j.biortech.2012.04.017
58. Majhi K, Let M, Halder U, et al. (2023) Copper adsorption ootentiality of bacillus stercoris GKSM6 and pseudomonas alcaliphila GKSM11 isolated from Singhbhum copper mines. *Geomicrobiol J* 40: 193–202. https://doi.org/10.1080/01490451.2022.2137603

59. Mekuto L, Ntwampe SKO, Jackson VA (2015) Biodegradation of free cyanide and subsequent utilisation of biodegradation by-products by Bacillus consortia: Optimisation using response surface methodology. *Environ Sci Pollut R* 22: 10434–10443. https://doi.org/10.1007/s11356-015-4221-4
60. Naguib MM, Khairalla AS, El-Gendy AO, et al. (2019) Isolation and characterization of mercury-resistant bacteria from wastewater sources in Egypt. *Can J Microbiol* 65: 308–321. https://doi.org/10.1139/cjm-2018-0379
61. Matsui K, Yoshinami S, Narita M, et al. (2016) Mercury resistance transposons in Bacilli strains from different geographical regions. *FEMS Microbiol Lett* 363: fnw013. https://doi.org/10.1093/femsle/fnw013
62. Chang CC, Lin LY, Zou XW, et al. (2015) Structural basis of the mercury(II)-mediated conformational switching of the dual-function transcriptional regulator MerR. *Nucleic Acids Res* 43: 7612–7623. https://doi.org/10.1093/nar/gkv681
63. Sone Y, Uraguchi S, Takanezawa Y, et al. (2017) Cysteine and histidine residues are involved in Escherichia coli Tn21 MerE methylmercury transport. *FEBS Open Bio* 7: 1994–1999. https://doi.org/10.1002/2211-5463.12341
64. Wahba HM, Lecoq L, Stevenson M, et al. (2016) Structural and biochemical characterization of a copper-binding mutant of the organomercurial lyase MerB: Insight into the key role of the active site aspartic acid in Hg-Carbon bond cleavage and metal binding specificity. *Biochemistry* 55: 1070–1081. https://doi.org/10.1021/acs.biochem.5b01298
65. Gätjens DR, Schweizer PF, Jiménez KR, et al. (2022) Methylotrophs and hydrocarbon-degrading bacteria are key players in the microbial community of an abandoned century-old oil exploration well. *Microb Ecol* 83: 83–99. https://doi.org/10.1007/s00248-021-01748-1
66. Pandit B, Moin A, Mondal A, et al. (2023) Characterization of a biofilm-forming, amylase-producing, and heavy-metal-bioremediating strain Micrococcus sp. BirBP01 isolated from oligotrophic subsurface lateritic soil. *Arch Microbiol* 205: 351. https://doi.org/10.1007/s00203-023-03690-x
67. Mishra S, Lin Z, Pang S, et al. (2021) Recent advanced technologies for the characterization of xenobiotic-degrading microorganisms and microbial communities. *Front Bioeng Biotech* 9. https://doi.org/10.3389/fbioe.2021.632059